Neutron dose estimation via LET spectrometry using CR-39 detector for the reaction ^{9}Be (p, n)

G. S. Sahoo, S. P. Tripathy, S. Paul, S. D. Sharma[1], S. C. Sharma[2], D. S. Joshi, T. Bandyopadhyay

Health Physics Division, [1]Radiological Physics and Advisory Division, [2]Nuclear Physics Division, Bhabha Atomic Research Centre, Mumbai, Maharashtra, India

ABSTRACT

CR-39 detectors, widely used for neutron dosimetry in accelerator radiation environment, have also been applied in tissue microdosimetry by generating the linear energy transfer (LET) spectrum. In this work, the neutron dose has been estimated via LET spectrometry for ^{9}Be (p, n) reaction which is useful for personnel monitoring around particle accelerators and accelerator based therapy facilities. Neutrons were generated by the interaction of protons of 6 different energies from 4–24 MeV with a thick Be target. The LET spectra were obtained from the major and minor radii of each track and the thickness of removed surface. From the LET spectra, the absorbed dose (D_{LET}) and the dose equivalent (H_{LET}) were estimated using Q-L relationship as given by International Commission on Radiological Protection (ICRP) 60. The track density in CR-39 detector and hence the neutron yield was found to be increasing with the increase in projectile (proton) energy. Similar observations were also obtained for absorbed dose (D_{LET}) and dose equivalents (H_{LET}).

Key words: LET spectrometry; ^{9}Be (p, n) reaction; CR-39; neutron dosimetry

Introduction

CR-39 detectors are widely used as neutron dosimeter in complex radiation fields such as particle accelerator radiation environment,[1] space stations in low earth orbit (LEO),[2] etc., because of their insensitivity to low Linear Energy Transfer (LET) radiations and convenient to expose, process and analyze. In an accelerator radiation environment, especially in a positive ion accelerator of intermediate energy, neutron is the dominant radiation produced during the interaction of ion with the target.[3] This is due to the interaction of projectile ions with the elements of surrounding materials forming a composite system whose mass, energy and number of nucleons depend on those of the projectile and the target material. This composite system goes to an excited state with a number of allowed decay channels to produce neutrons depending on the excitation energy of the system.[4] The energy and yield of the emitted neutrons depend on the type and energy of the projectile and type of the target.[5] However, in case of medical applications such as boron neutron capture therapy (BNCT)[6,7] higher neutron yield is required, which is a binary radiotherapy method used for treatment of brain tumour. In this regard, the accelerator based neutron sources (ABNS)[8] are preferred to provide required flux of neutrons necessary for treatment purpose. The commonly used projectiles for ABNS are proton (^{1}H) and deuteron (^{2}H) with different targets such as deuteron (^{2}H), tritium (^{3}H), ^{7}Li, ^{9}Be, etc., and are being researched worldwide.[9-11] Owing to the increasing demand of more powerful accelerators for various applications such as industrial, medical or research purposes and also increase in the number of workers in these radiation fields, the techniques and methodologies for neutron dosimetry are continuously being improved. It is important to mention that, measurement and/or estimation of neutron dose in such radiation environments are critical for radiation protection of occupational workers during normal operating as well as accidental situations.

Neutron dose estimation using CR-39 detectors are usually performed by the following approaches: (1) Correlation of track density with established calibration factors obtained

Address for correspondence:
Dr. S. P. Tripathy,
Room No. 510, CT and CRS Building,
AERB Complex, Anushaktinagar,
Mumbai - 400 094, Maharashtra, India.
E-mail: sam.tripathy@gmail.com

from the standard neutron sources,[12] (2) generation of the neutron spectrum from track parameters and then multiplying with the dose conversion coefficient[13-16], (3) measurement of optical absorbance and then correlating the changes in absorbance with neutron dose.[17] Each method has its inherent advantages and limitations, but can always serve as complementing to other methods if any of the techniques fail under typical radiation environments. LET spectrometry method using CR-39 detectors[18,19] is also another way of estimating neutron dose, which is useful in situations when the information about neutron energy distribution and the radiation components are not available. In this approach, the discrimination of different radiation components (such as proton, carbon and oxygen) due to neutron interaction in CR-39 is not required. Furthermore, this LET spectrum is crucial for determining the energy deposition in microscopic level and to estimate the absorbed dose (D_{LET}) and dose equivalent (H_{LET}). Since the composition of CR-39 is similar to that of human tissue, it is reasonable to consider that the dose delivered in CR-39 is equivalent to that in tissue. However, different radiation components do have different contribution to the total dose depending on their LET values.

In this work, CR-39 detectors were used to measure the LET spectrum and to estimate the neutron dose for the ⁹Be (p, n) reaction at different proton energies from 4–24 MeV. The ⁹Be (p, n) reaction is chosen because of its importance for producing fast neutrons at relatively higher yield[20] which is suitable for BNCT application.[11,21,22]

Materials and Methods

Irradiation

The CR-39 detectors (12 mm × 12 mm × 1.5 mm, Intercast, Parma, Italy) were irradiated to neutrons generated from the interaction of protons with a thick ⁹Be target at the 6 m irradiation port above the analyzing magnet of BARC-TIFR Pelletron Accelerator facility. The irradiation was performed along the beam direction at a distance of 1.75 cm from the 6 mm thick Be target. The projectile (proton) energies used in this study were 4, 8, 12, 16, 20 and 24 MeV. The detectors were exposed for 1 minute duration at 70 nA beam current which was found to be sufficient to produce statistically significant number of tracks. A current integrator was attached to the target to measure the total accumulated charge on the target from which the number of protons hitting the target was found out. Details of the irradiation parameters are given in Table 1.

Track development and image analysis

After irradiation, the initial thicknesses of the detectors were measured using a precision thickness gauge (Model: FT3, Hanatek, East Sussex, UK) with resolution of 0.1 µm. Then the neutron induced latent tracks produced in CR-39 detectors were developed by chemical etching (6.25 N NaOH,

Table 1: Beam parameters during irradiation

Proton energy (MeV)	Beam current (nA)	Total charge on target (µC)	Number of protons on target (×10¹⁴)
4	70	43.2	2.69
8	70	45.6	2.85
12	70	44.0	2.75
16	70	43.3	2.70
20	70	40.9	2.55
24	70	42.7	2.66

70°C, 6h). After etching, the final thicknesses of the detectors were measured. The images of developed tracks were captured by manually selecting undamaged frames using an optical microscope (Model: Axio Scope A1, Carl Zeiss, Germany) at a microscopic magnification of 200x. The captured images were analysed using the image analyzing software Axiovision 4.8. All the 2-dimensional track parameters, such as track area, diameter, major and minor radii, grey level, feret length, perimeter, etc., were automatically obtained by the software, out of which the major and minor radii of all the counted tracks were considered to determine the etch rate ratio (V) which is the ratio of track etch rate (V_t) to bulk etch rate (V_b). Another pristine detector was processed in similar procedure to subtract the background contribution.

Generation of V spectrum and LET spectrum

The V was calculated from the major and minor radii using the formulation[23] given below.

$$\tan\phi = \frac{T}{2a}\left[1 - \frac{b^2}{T^2}\right] \tag{1}$$

$$V = \frac{V_t}{V_b} = \frac{1}{\sin\phi} \tag{2}$$

where ϕ is the cone angle of the track, *a* and *b* are major and minor entrance radii of tracks, *T* is the thickness of removed surface from each side of the detector due to etching. From the distribution of V of the tracks, the V spectra were obtained for the neutrons emitted from ¹H + ⁹Be reaction. The V spectra were then converted to LET spectra using the calibration curve reported in the literature[24] which correlates the V values to LET in water. From the LET spectra, the absorbed dose (D_{LET}) and the dose equivalent (H_{LET}) were obtained for ⁹Be (p, n) reaction at different proton energies from 4-24 MeV.

Results and Discussion

Figure 1 shows the microphotographs of an unirradiated CR-39 and the neutron induced recoil tracks produced by ⁹Be (p, n) reactions at different proton energies. As shown in the figure, number of tracks was found to be less in case of 4 MeV protons while more number of tracks appeared in
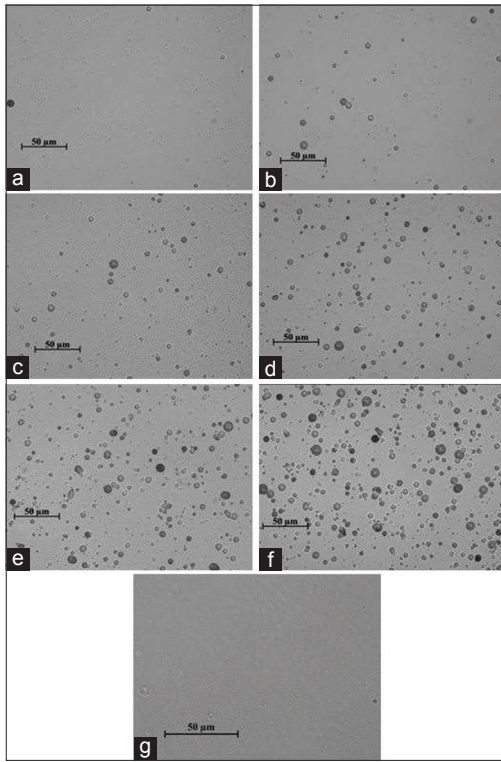
Figure 1: Microphotographs of developed recoil tracks produced by neutrons from (a) 4, (b) 8, (c) 12, (d) 16, (e) 20 and (f) 24 MeV protons with Be target along with (g) background tracks

Figure 2: Variation of neutron-induced recoil track density with proton energy. The projectiles (proton) of different energies from 4-24 MeV were bombarded on a thick Be target to produce neutrons

case of 24 MeV protons indicating higher neutron yield at higher projectile energies.

As the energy of the proton increases, the tail end of the neutron spectrum spreads towards higher energy contributing to higher neutron yield, thereby forming more number of tracks in the CR-39 detector. Nevertheless, the tracks were found to be of different shapes and sizes depending on the recoil angle and energy of the ions within the detector. The track density (number of tracks per unit area) in CR-39 is plotted versus projectile (proton) energy in Figure 2. The track density presented in Figure 2 was obtained after subtracting background track density (which is about 1800 tracks cm^{-2}) from the total number of tracks. It is observed from the figure that, the track density increased almost linearly with the proton energy.

Figure 3 shows the variation of the track major radii to the minor radii at all the proton energies. As seen from Figure 3, the tracks near the 45° line represent the circular tracks whereas the tracks above the line are the elliptical tracks. Circular tracks were found to be more than the elliptical tracks for all energies except 24 MeV protons. The ratio of circular to elliptical tracks were found to be about 1.91 at 4 MeV and decreased upto about 0.87 at 24 MeV.

Using the equation 1 and 2 given above, the V value was obtained from major and minor radius of each track from

which the V spectra were generated for all the detectors. Figure 4 shows the unit V spectra obtained for all the detectors irradiated with neutrons produced by ^{9}Be (p, n) reaction at all the proton energies used in this study. The unit spectrum was generated by dividing the track density in each bin by the total track density. The V values beyond 5.05 were not considered due to insignificant number of counts.

The LET spectra from 12 keV/μm to 330 keV/μm obtained from the V spectra are shown in Figure 5. As observed from Figure 5, the track density per proton at each LET interval was found to be lowest at 4 MeV protons and was found to be increasing with proton energy. However, a few overlapping regions were observed towards higher LET values where the statistical fluctuations appeared due to the less number of track density in higher LET bins. This observed fluctuation was mainly due to the recoil carbon and oxygen ions having less number of counts. However, their contribution to dose is significant because of their high LET values. The larger contribution towards lower values of the LET spectra was due to the neutron induced recoil protons within the detector.

The dose characteristics (D_{LET}, H_{LET}) of secondary particles due to neutrons were determined from the measured LET spectra using the formulations[25]

$$D_{LET} = \int (dN/dL)LdL \qquad (3)$$

$$H_{LET} = \int (dN/dL)LQ(L)dL \qquad (4)$$

where dN/dL is the number of tracks per unit area in a LET interval and L is the value of LET. $Q(L)$ is the quality factor given in ICRP 60.[26] The absorbed dose (D_{LET}) and dose equivalent (H_{LET}) per proton obtained from
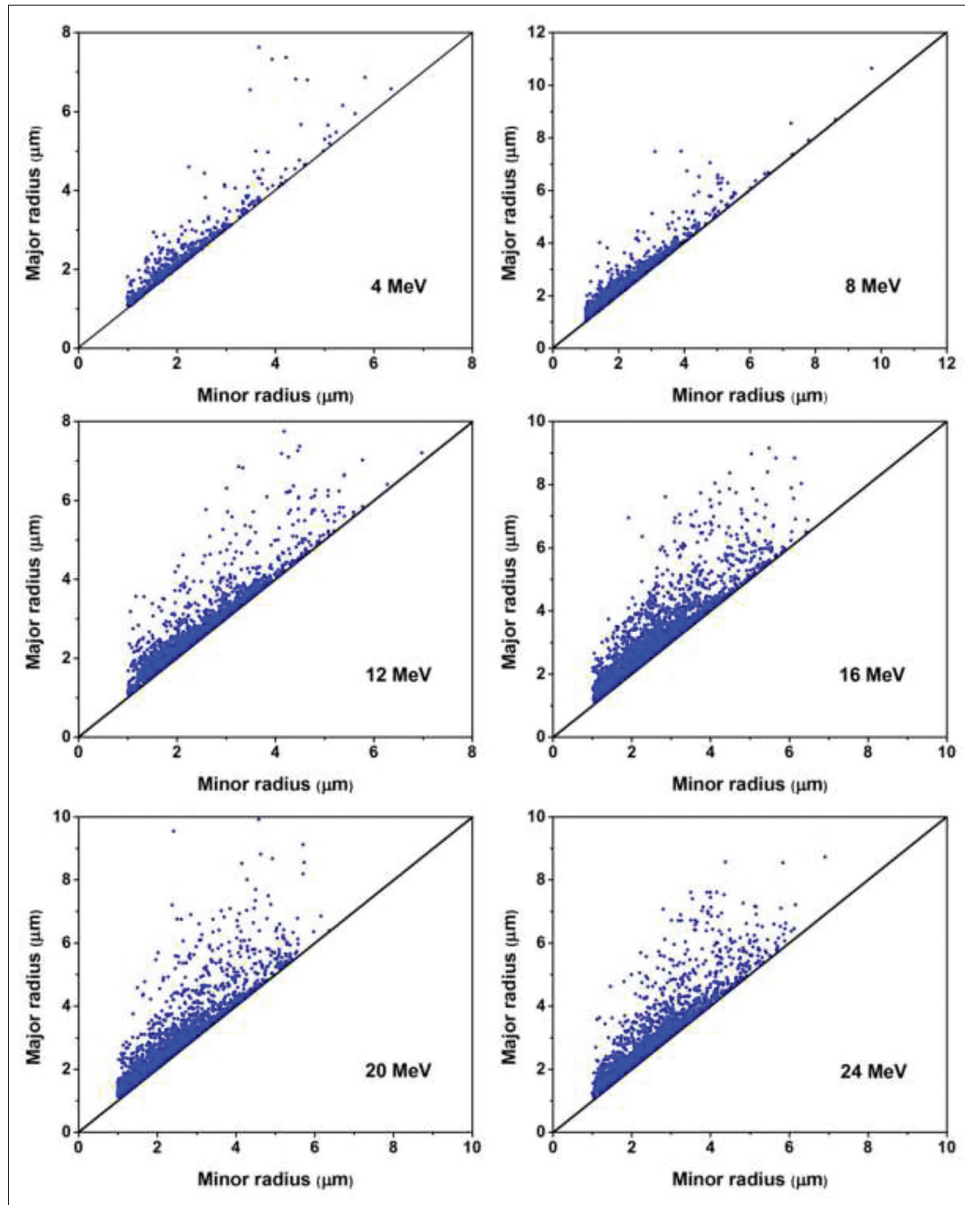
Figure 3: Variation of track major radius with minor radius at all the proton energies. The tracks near the solid line at 45° are circular and rest tracks are elliptical with different degree of ellipticity

LET spectra is presented in Table 2. As can be seen form Table 2, the absorbed dose and dose equivalent per incident proton was found to be increasing with increase in proton energy. The microdosimetric distributions of absorbed dose and dose equivalent are presented in Figure 6 and 7 respectively. However, the absorbed dose and the dose equivalent estimated in the present work have large fluctuations beyond LET of about 200 keV/μm due to statistical uncertainty in the measurement of V_t/V_b and corresponding LET values.

Conclusion

The LET spectra from 12 keV/μm to 330 keV/μm were measured for the neutrons generated from the interaction

Table 2: Absorbed dose (D_{LET}) and Dose equivalent (H_{LET}) per proton obtained from LET spectra for different proton energy

Proton energy (MeV)	D_{LET} per proton (pGy)	H_{LET} per proton (pSv)
4	3.68×10^{-4}	5.34×10^{-3}
8	1.47×10^{-3}	2.27×10^{-2}
12	3.38×10^{-3}	4.63×10^{-2}
16	7.30×10^{-3}	9.66×10^{-2}
20	1.01×10^{-2}	1.46×10^{-1}
24	1.58×10^{-2}	2.77×10^{-1}

D_{LET}: Absorbed dose, H_{LET}: Dose equivalent, LET: Linear energy transfer

of proton with a thick Be target at different proton energies between 4 and 24 MeV. The track density was found to increase almost linearly with proton energy indicating
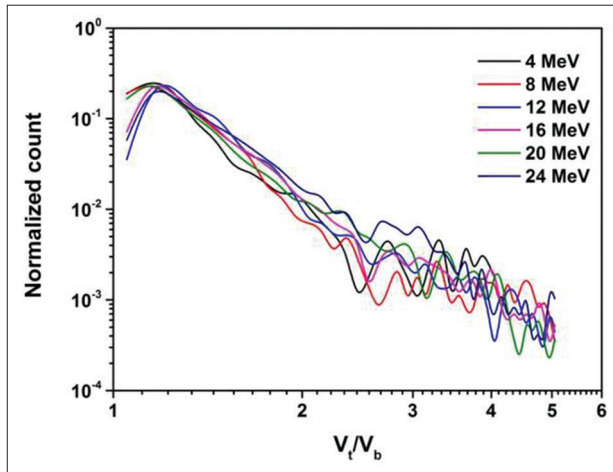
Figure 4: Unit etch rate ratio (*v*) spectra for neutrons produced by ⁹Be (p, n) reactions at different proton energies. Each spectrum is generated per unit track density
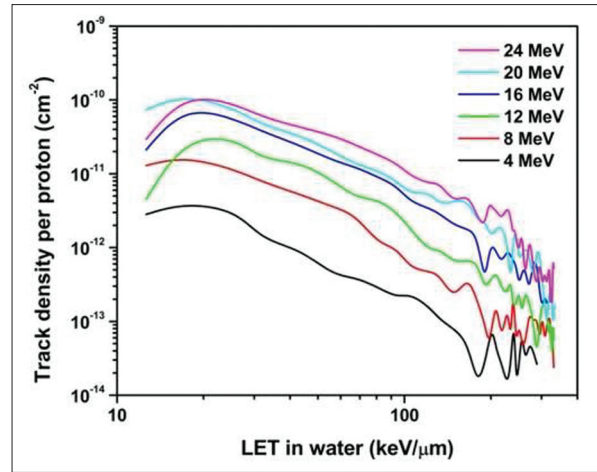
Figure 5: LET (Linear Energy Transfer) spectra for neutrons produced by 9Be (p, n) reactions at different proton energies
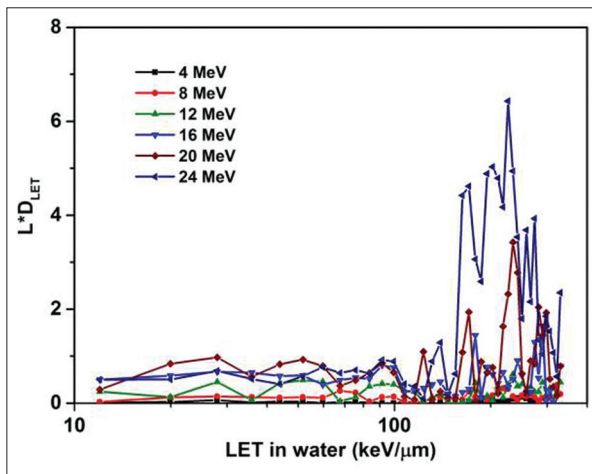
Figure 6: Microdosimetric distributions of absorbed dose as a function of LET
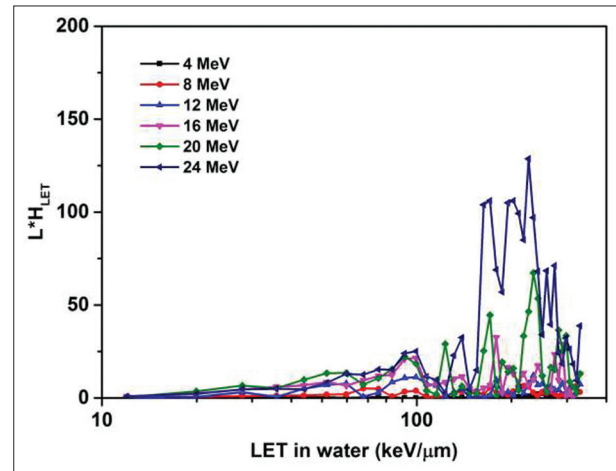
Figure 7: Microdosimetric distributions of dose equivalent as a function of LET

higher neutron yield at higher projectile energy. Similarly, the absorbed dose and the dose equivalent per incident proton were also found to be increasing with the proton energy. The dose values obtained in this study can be useful for personal neutron dosimetry in the accelerator environment.

Acknowledgements

References

1. Agosteo S. Overview of novel techniques for radiation protection and dosimetry. Radiat Meas 2010; 45:1171-7.
2. Satoshi K, Hajime K, Hisashi K, Mieko K, Yukio U, Nakahiro Y, *et al*. Analysis of radiation dose variations measured by passive dosimeters onboard the International Space Station during the solar quiet period (2007-2008). Radiat Meas 2013;49:95-102.
3. Patterson HW, Thomas RH. Accelerator Health Physics. New York: Academic Press; 1973
4. Sarkar PK. Neutron dosimetry in the particle accelerator environment. Radiat Meas 201045:1476-83.
5. Sarkar PK, Bandyopadhyay T, Muthukrishnan G, Ghosh S. Neutron production from thick targets bombarded by alpha particles: Experiment and theoretical analysis of neutron energy spectra. Phys Rev C Nucl Phys 1991;43:1855-66.
6. Barth RF, Coderre JA, Vicente MG, Blue TE. Boron neutron capture therapy of cancer: Current status and future prospects. Clin Cancer Res 2005;11:3987-4002.
7. IAEA-TECDOC-1223. Current status of neutron capture therapy. International Atomic Energy Agency 2001.
8. Blue TE, Yanch JC. Accelerator-based epithermal neutron sources

for boron neutron capture therapy of brain tumors. J Neurooncol 2003;62:19-31.

9. Faghihi F, Khalili S. Beam shaping assembly of a D–T neutron source for BNCT and its dosimetry simulation in deeply-seated tumor. Radiat Phys Chem 2013;89:1-13.

10. Fantidis JG, Saitioti E, Bandekas DV, Vordos N. Optimised BNCT facility based on a compact D-D neutron generator. Int J Radiat Res 2013;11:207-14.

11. Yoshikai K, Kenji A, Akihiro A, Shin F, Fujio H, Kenju, *et al*. A Project of boron neutron capture therapy system based on a proton linac neutron source. Phys Proc 2012;26:223-30.

12. Gisela SM, Lopez F, Bernaola OA. Neutron dosimetry device using PADC nuclear track detectors. J Radioanal Nucl Chem 2011;287:635-8.

13. Luszik-Bhadra M, Dietz E, D'Errico F, Guldbakke S, Matzke M. Neutron spectrometry with CR-39 track detectors and silicon diodes using unfolding techniques. Radiat Meas 1997;28:473-8.

14. D'Errico F, Weiss M, Luszik-Bhadra M, Matzke M, Bernardi L, Cecchi A. A CR-39 track image analyser for neutron spectrometry. Radiat Meas 1997;28:823-30.

15. Paul S, Tripathy SP, Sahoo GS, Bandyopadhyay T, Sarkar PK. Measurement of fast neutron spectrum using CR-39 detectors and a new image analysis program (autoTRAK_n). Nucl Instrum Meth Phy Res A 2013;729:444-50.

16. Tripathy SP, Paul S, Sahoo GS, Suman V, Sunil C, Joshi DS, *et al*. Measurement of fast neutron spectra generated from the interaction of 20 MeV protons with thick Be and C targets using CR-39 detector. Nucl Instrum Meth Phy Res B 2014;318:237-40.

17. Sahoo GS, Paul S, Tripathy SP, Sharma SC, Jena S, Rout S, *et al*. Effects of neutron irradiation on optical and chemical properties of CR-39: Potential application in neutron dosimetry. Appl Radiat Isot 2014;94C: 200-5.

18. Spurny F, Bednar J, Johansson L, Satherberg A. Linear ener*gy* transfer spectra of secondary particles in CR-39 track etch detectors. Radiat Meas 1996;26:645-9.

19. Sahoo GS, Tripathy SP, Sunil C, Sarkar PK. LET spectrometry of 14 MeV (D-T) neutrons using CR-39 track detectors. Nucl Instrum Meth Phy Res A 2013;708:46-50.

20. Paul S, Sahoo GS, Tripathy SP, Sharma SC, Ramjilal, Ninawe NG, *et al*. Measurement of neutron spectra generated from bombardment of 4 to 24 MeV protons on a thick 9Be target and estimation of neutron yields. Rev Sci Instrum 2014;85:063501-1-7.

21. Kobayashi H, Kurihara T, Matsumoto H, Yoshioka M, Kumada H, Matsumura A *et al*. Construction of a BNCT Facility Using an 8-MeV High Power Proton LINAC in Tokai. Proceed. of IPAC. New Orleans, Louisiana, USA; 2012.

22. Tanaka H, Sakurai Y, Suzuki M, Masunaga S, Kinashi Y, Kashino G, *et al*. Characteristics comparison between a cyclotron-based neutron source and KUR-HWNIF for boron neutron capture therapy. Nucl Instrum Meth Phy Res B 2009;267:1970-7.

23. Charvat J, Spurny F. Optimization of etching characteristics for celluose nitrate and CR-39 track detectors. Int J Radiat Appl Instrum D 19 88;14:447-9.

24. Spurny F, Molokanov AG, Bamblevski VP. Passive spectrometry of linear energy transfer: Development and use. Radiat Prot Dosimetry 2004;104:675-9.

25. Ghergherehchi M, Afarideh H, Kim YS, Park SY, Lee SB, Shin DH, *et al*. Dosimetry and microdosimetry of 10-220 MeV proton beams with CR-39 and their verifications by calculation of reaction cross sections using ALICE, TALYS and GEANT4 codes. Radiat Meas 2012;47:410-6.

26. ICRP, 1991. Recommendations of the International Commission on Radiological Protection. ICRP Publication 60. Ann. ICRP 21 (1-3);1990.